HHS Public Access

Author manuscript

Dev Neurosci. Author manuscript; available in PMC 2018 March 18.

Published in final edited form as:

Dev Neurosci. 2017 ; 39(1-4): 66–81. doi:10.1159/000456030.

Proteomic analysis of mouse cortex postsynaptic density following neonatal brain hypoxia-ischemia

Guo Shao[1,*], **Yongqiang Wang**[2,*], **Shenheng Guan**[3,*], **Alma L Burlingame**[3], **Fuxin Lu**[4], **Renatta Knox**[5], **Donna M Ferriero**[4,6], and **Xiangning Jiang**[4]

[1]Department of Biochemistry, Baotou Medical College, Inner Mongolia, China

[2]Department of Cellular & Molecular Pharmacology, University of California San Francisco, CA, USA 94143

[3]Department of Pharmaceutical Chemistry, University of California San Francisco, CA, USA 94143

[4]Department of Pediatrics, University of California San Francisco, CA, USA 94143

[5]Department of Pediatrics, Weill Cornell Medical College, New York, NY, USA 10065

[6]Department of Neurology, University of California San Francisco, CA, USA 94143

Abstract

Proteomics of the synapses and postsynaptic densities (PSDs) have provided a deep understanding of protein composition and signal networks in adult brain, which underlie neuronal plasticity and neurodegenerative or psychiatric disorders. However, there is a paucity of knowledge about the architecture and organization of PSDs in the immature brain, and how it is modified by brain injury in early developing stage. Mass spectrometry (MS)-based proteomic analysis was performed on PSDs prepared from cortices of postnatal day 9 naïve mice or pups suffered hypoxic-ischemic (HI) brain injury. 512 proteins of different functional groups were identified from PSDs collected from naive animals, among which 60 have not been reported previously. Seven newly identified proteins involved in neural development were highlighted. HI increased the yield of PSDs at early time points upon reperfusion, and multiple proteins were recruited into PSDs following the insult. Quantitative analysis was preformed using spectral counting, and proteins whose relative expression was more than 50% up- or down-regulated compared to the sham animals at 1hr after HI were reported. Validation with Western blotting demonstrated changes in expression and phosphorylation of the NMDA receptor, activation of a series of postsynaptic protein kinases and dysregulation of scaffold and adaptor proteins in response to neonatal HI. This work, along with other recent studies of synaptic protein profiling in the immature brain, builds a foundation for future investigation on the molecular mechanisms underlying developing plasticity. Furthermore, it provides insights into the biochemical changes of PSDs following early brain hypoxia-ischemia, which is helpful for understanding not only the

Corresponding author: Xiangning Jiang, Department of Pediatrics, University of California, San Francisco 675 Nelson Rising Lane Room 494, San Francisco, CA 94158, Phone: 415-502-7278, Fax: 415-502-7325, xiangning.jiang@ucsf.edu.

*These authors contributed equally to this work

injury mechanisms, but also the process of repair or replenishment of neuronal circuits during recovery from brain damage.

Keywords

brain; development; hypoxia/ischemia; proteomics

Introduction

Synaptogenesis and experience-based synaptic changes after birth and during critical periods are important component of brain development. One distinct marker of synapse maturation is postsynaptic specializations and the appearance of postsynaptic densities (PSDs) at excitatory synapses. Neurotransmitter receptors are enriched and linked to cytoskeleton and signaling molecules at PSDs, which enables information transmission between neurons. Activity-dependent dynamic changes in the protein components of the PSDs are molecular basis of synaptic plasticity and cognitive function. Brain injury in early postnatal life, including hypoxia-ischemia (HI), could affect PSDs/synapse maturation and thereby disrupt brain development.

The structure and protein composition of the PSDs have been studied in great detail in adult rodent (mouse and rat) brain during the past 15 years. The advances in mass spectrometry (MS)-based large-scale proteomics and phosphoproteomics have enabled the identification and quantification of hundreds to more than 2,000 PSD proteins and their posttranslational modifications [1–7]. These studies unraveled not only the postsynaptic organization of synapses, but also the signaling networks driven by neurotransmitter receptor activation [8,9]. They greatly enhanced our understanding of synaptic plasticity and related neurodegenerative or psychiatric disorders. However, quantitative proteomic analysis of the highly malleable developing brain and the knowledge about temporal changes in PSD profiles during brain development, as well as its alterations in response to neonatal encephalopathy, including neonatal HI, is very limited.

Age-related proteomic studies revealed a list of proteins that are differentially expressed or phosphorylated in neonatal and adult mouse brain [10–15]. The higher levels of proteins in the developing brain are mostly involved in neurogenesis, neuronal migration or neurite outgrowth. To date, there are less than five MS-based proteomic studies that were performed in neonatal (postnatal day 3 or 7) HI model, all of which used proteins extracted from entire brain or cortex or hippocampus without further fractionation [16–19], a comprehensive proteomic profiling of PSD proteins in the developing brain is still lacking.

The present study provides a global characterization of PSD proteins purified from neonatal C57Bl6 mouse cortex at postnatal day 9 (P9), a developing stage that is equivalent to term human infants. A total of 512 proteins were identified, which are classified into different functional categories, including 60 proteins that have not been reported in previous synapse proteomic studies with adult and developing brain. In addition, we listed proteins that were newly recruited to PSD or were more than 50% up-or down-regulated at 1 hour after HI compared to their sham-operated littermates. HI-induced molecular modifications of PSDs

may be associated with signaling pathways leading to neuronal death/survival and early disturbance of synaptic plasticity and brain development in term babies with hypoxic-ischemic encephalopathy.

Materials and Methods

All animal experiments were approved by the University of California San Francisco (UCSF) institutional animal care and use committee. C57BL/6 mice (Simonsen) with litters were allowed food and water *ad libitum*. Both sexes were used for these studies at postnatal day 9 (P9).

Neonatal Brain Hypoxic-Ischemic (HI) Injury

Neonatal HI was performed as previously described with the Vannucci procedure [20]. At P9, pups were anesthetized with isoflurane (2–3% isoflurane/balance oxygen) and the left common carotid artery was electrocauterized. Animals were allowed to recover for one hour with their dam and then exposed to 60 minutes of hypoxia in a humidified chamber at 37°C with 10% oxygen/balance nitrogen. Sham-operated control animals received isoflurane anesthesia and exposure of the left common carotid artery without electrocauterization or hypoxia. HI and sham animals were returned to their dams until they were euthanized.

PSD sample preparation

Purification of PSD-associated synaptic proteins was carried out as described using a subcellular fractionation approach followed by extraction with Triton X-100 [21,22]. Cortical tissue was homogenized in ice-cold sucrose buffer containing 0.32M sucrose, 10mM Tris-HCl (pH 7.4), 1mM EDTA, 1mM EGTA and protease and phosphatase inhibitors (Complete mini and Phospho-Stop cocktail tablets, Roche, Indianapolis, IN). A low-speed (1,000×*g*) centrifugation was performed to remove the nuclear fraction and tissue debris. The resulting supernatant (S1) was spun at 10,000×*g* for 15 minutes to yield a crude membrane fraction (P2). The supernatant (S2) was then centrifuged at 100,000×g for 60 min to separate cytoplasmic protein (S3) and intracellular light membrane fraction (P3). The P2 was subsequently resuspended in 120 μl sucrose buffer, and mixed with 8 volumes of 0.5% Triton X-100 buffer containing 10mM Tris-HCl (pH 7.4), 1mM EDTA, 1mM EGTA and protease and phosphatase inhibitors. The mixture was homogenized again with 30 pulses of a glass pestle and rotated at 4°C for 30 min followed by centrifugation at 32,000×g for 30 min in a TL-100 tabletop ultracentrifuge (Beckman). The resultant pellet containing Triton X-insoluble postsynaptic density (PSD) proteins were dissolved in TE buffer (100 mM Tris-HCl, 10mM EDTA) with 0.5% SDS and stored at −80 °C until use. Protein concentration was determined by the bicinchoninic acid method (Pierce). The purity of PSD was verified by Western blots as described [21].

LC-MS/MS analysis and protein identification

Fifteen μg of PSD protein mixture was precipitated overnight at −20°C with addition of 4× volume of ice-cold acetone. After centrifugation, the pellet was redissolved and reduced in 9μl of 50mM ammonium bicarbonate (ABC) solution containing 8M urea and 10mM tris (2-carboxyethyl) phosphine (TCEP) at 37°C followed by alkylation with 20mM

chloroacetamide in the dark at room temperature. The sample was diluted with 50mM ABC solution at least 4 times to make the final concentration of urea less than 2M and then proceeded to in-solution digestion with combined trypsin (sequencing grade, Promega) and lysyl endopeptidase C (Lys-C, mass spectrometry grade, Wako) at the ratio of enzyme : protein of 1:25 in mass. After incubation at 37 °C for 16 hours, the digested peptides were extracted and desalted with C18 solid phase extraction tip (10ul bed C18 ZipTip, Pierce) and then eluted with two sequential 10ul aliquots of 50% acetonitrile in 0.1% trifluoroacetic acid. The combined elute was dried in Speed Vac and resuspended in 0.1% formic acid/2% acetonitrile for MS analysis.

The peptides were analyzed by LC-MS/MS on LTQ Orbitrap mass spectrometer (ThermoFisher Scientific, San Jose, CA) equipped with a Waters NanoAcquity LC system (Milford, MA) at UCSF Mass Spectrometry Facility. Peptides were separated on an Easy-Spray column (Thermo, PepMap, C18, 3μm, 100Å, 75μm × 15cm) using a linear gradient from 2% solvent A (0.1% formic acid in water) to 25% solvent B (0.1% formic acid in acetonitrile) at 300 nL/min over 47 min. MS precursor spectra were measured in the Orbitrap from 300–2000 *m/z* at 30,000 resolving power, top six precursor ions were selected and dissociated by collision-inducedl dissociation (CID) for MS/MS. The MS/MS data were searched against mouse protein sequences in the SwissProt database (downloaded from Uniprot on 2015.10.12) using MSGF+ search engine [23] with a concatenated database consisting of normal and randomized decoy databases. The false discovery rates for peptide identification were estimated to be 1.2%, corresponding to maximum expectation value of 0.102. Parent/precursor mass tolerance and fragment mass tolerance were 20ppm and 0.6 Da, respectively. Constant modification of carbamidomethylation on cysteine (C) and variable modifications of deamidation of N-terminal glutamine, initial protein methionine loss with or without N-terminal acetylation were employed.

Semi-quantification of PSD proteins using spectral counting

A semi-quantitative analysis was performed using spectral counting, which relies on the number of peptides (peptide count) identified from a given protein. This simple label-free quantification technique is based on the observation that the more abundant a protein is, the more peptides can be identified from it. It provides a tool for rapid screening and broad estimation of relative protein amount between samples [24]. For each protein, the mean peptide counts and standard deviations (SD) from triplicate analysis (three repeated LC/MS/MS analysis of the same sample) of naïve, sham and HI group were determined and their 95% confidence intervals were calculated with the formula: mean ±1.96*(SD/√n), in which SD and n (=3) are the standard deviation and the number of replicates, respectively. The mean ratio (fold change) of HI/sham was used to represent differential expression of each protein after HI, and 95% confidence interval of the ratio was reported to indicate reliability of the results.

Western blotting of PSD samples

For Western blot analysis, an equal amount of PSD protein samples (5μg) was applied to 4–12% Bis-Tris SDS polyacrylamide gel electrophoresis and transferred to polyvinyl difluoride membrane. The blots were probed with the primary antibodies (listed in

Supplemental Table S2) overnight at 4°C. Appropriate secondary horseradish peroxidase-conjugated antibodies (Santa Cruz Biotechnology Inc.) were used, and signal was visualized with enhanced chemiluminescence (Amersham, GE Healthcare). Image J software was used to measure the mean optical densities (OD) and areas of protein signal on radiographic film after scanning.

Statistical Analysis

Proteins detected by MS experiments were semi-quantified using spectral counting from triplicate MS run of 2 sets of samples of each group. The differences of relative protein expression are presented as mean ratio (fold change) of HI/sham counts and mean confidence interval of the ratio. Data of optical densities of immunoblots are presented as mean ± SD and were evaluated statistically using SAS Wilcoxon-Mann-Whitney test. Differences were considered significant at $p < 0.05$.

Results

Identification of PSD proteins in neonatal mouse brain

To study the protein composition of PSDs in the immature brain, PSD fractions were purified from naïve P9 C57BL/6 mouse cortices. A short protocol published previously [21,22] was utilized instead of the original method of Carlin *et al.*, which employed a long two-step sucrose density gradient centrifugation procedure [25]. The PSD-associated proteins prepared with this protocol had similar migration profiles in Coomassie blue-stained SDS-PAGE gel (Fig. 1B) to those isolated from adult brain, and the purity was comparable to that extracted with the original Carlin method [26]. After in-solution digestion and LC-MS/MS analysis/database search, a total of 512 proteins were identified, all of which were categorized in different groups based on their published biological functions (complete list in Supplemental Table S1). The false positive rate for the database search was estimated to be ≈ 1.2% with the maximal peptide expectation value (e-value) of 0.102. The e-value threshold was determined based on the distributions of e-values (ev) of spectra matched against the normal SwissProt database and matched against the randomized version of the normal database (Fig. 1C). The identified proteins were reported with their name, UniPro accession number, the number of unique peptides used to identify the protein, the percent sequence coverage for each protein, and the best expectation values for the most confident peptide identification for each protein. Similar to reports from adult PSD proteomic studies, the proteins fell into major categories of receptors/channels/transporters; scaffold/adaptors/trafficking proteins; kinases/phosphatases and regulators; cytoskeleton/motor and modulators; small G-proteins/GTPases/ATPases; and adhesion/chaperon proteins [1,2,4–6,27]. It is not surprising that a large amount of ribosomal proteins, elongation factor 1 and heterogeneous nuclear ribonucleoproteins (hnRNP) were detected indicating active local protein translation/synthesis at or proximal to PSDs [1,4,5]. Proteins from presynaptic sites (protein bassoon, piccolo, synapsin, etc.); from mitochondria and nuclei have been frequently identified in postsynaptic proteomic experiments [4,5,27]. Interestingly, a previous study showed that RNA binding protein hnRNP A3 that was also found in this study, was localized in both nucleus and spines [2]. Other identified hnRNP A1, A2/B1, A3, L, M, were demonstrated to accumulate at PSDs with synaptic activity [28]. Some of the

known PSD proteins that were not detected in the MS experiments are likely to be low in abundance.

Newly identified PSD proteins that regulate neural development

To discover the novel proteins that have not been reported in previous synapse proteomic studies, proteins identified in this work were compared to published data from six other proteomic experiments with the PSD or synaptic membrane fractions [1,4,5,7,13,27]. Of the 512 proteins identified with high confidence, 452 were detected in mature or immature synapses by MS, while 60 have not been reported in previous PSD or synapse proteomes (underlined in Supplemental Table S1). Seven novel proteins with functions in neural development are highlighted (Table 1). Breast cancer type 2 susceptibility protein homolog (BRCA2) is known to be a tumor suppressor involved in repair of DNA double-strand breaks. It is required for neurogenesis during embryonic and postnatal neural development whose deficiency leads to increased apoptosis and microcephaly [29]. Charged multivesicular body protein 1a (CHMP1A) was originally identified as a member of the ESCRT-III endosomal sorting complex that assists in the trafficking of ubiquitinated cargo proteins to the lysosome for degradation [30]. It also localizes to the nuclear matrix and regulates chromatin structure [31]. A recent study demonstrated its involvement in neural progenitor cell proliferation and cerebellar development [32]. C-Jun-amino-terminal kinase-interacting protein 1 (JIP1) is a scaffold protein that activates JNK cascade pathways, and an adaptor linking cargo to Kinesin-1, a major motor protein for axonal transport. It is highly expressed in neurons and through interplay with AKT, promotes axonal growth in cortical cultures [33,34]. In vivo, it is important for polarization and migration of cortical neurons [35]. Serine/threonine-protein kinase MARK1 (microtubule affinity-regulating kinase 1) encodes a kinase-regulating microtubule-dependent transport in axons and dendrites [36]. It is a polarity protein implicated in axon-dendrite specification and neurite outgrowth [37,38]. MARK1 is involved in neuronal migration by phosphorylating doublecortin, MAP2 and tau [39]. Through phosphorylating PSD95 [40] or DIX domain containing 1 (DIXDC1) [41], MARK1 plays essential roles in dendritic spine morphogenesis. It is overexpressed in the prefrontal cortex of autistic patients and proposed as a susceptibility gene for autism [37]. Two other proteins regulate neurite outgrowth with opposite effects. Probable global transcription activator SNF2L1, a chromatin remodeling protein, is enriched in the brain and potentiates neurite outgrowth [42], while toll-like receptor 3 (TLR3), an innate immunity receptor usually found in glial cells, acts as a negative regulator of axonal growth [43]. SNF2L is also found to inhibit progenitor cell expansion and promote neuronal differentiation in the developing brain [44]. TLR3 is strongly expressed in the brain during early embryogenesis and decreases in postnatal period [45]. It constrains proliferation of embryonic neural progenitor cells and adult hippocampal neurogenesis [45,46]. In adult brain, TLR3 signaling reduces hippocampus-dependent learning and memory and AMPA receptor expression in CA1 neurons [46]. Sec 14 domain and spectrin repeat-containing protein 1 (SESTD1) is a binding partner of group 4 calcium-permeable transient receptor potential channels TRPC4 and TRPC5 [47]. In vitro studies suggested that SESTD1 negatively regulates dendritic spine density and reduces excitotory synaptic transmission in cultured hippocampal neurons [48]. It may play a role in synapse formation or maturation

given its residence at PSD and being more prevalent during embryogenesis and early postnatal weeks [48].

Increase of PSD yield and recruitment of proteins into PSD in response to neonatal HI

To investigate the early responses of postsynaptic protein machinery to hypoxia-ischemia, PSD fractions were purified from sham-operated control mice and mice subjected to 60 min of HI, followed by 15min and 1 hour of reperfusion. There was an increase of PSD yield at these early time points (by 51.23% at 15min and 14.94% at 1hr, n = 8–9, Fig.1D). The yield of PSDs was 1.218 ± 0.16 μg per mg cortical tissue in sham brains, 1.842 ± 0.173 μg/mg at 15min after HI ($p < 0.05$), and 1.4 μg/mg at 1hr after HI. There were no differences in the yield of intracellular light membrane and cytoplasmic protein fractions following HI (Fig. 1D).

The MS-based proteomic experiments with PSDs from sham and HI-injured animals provided an overall picture of the alterations in PSD protein composition. Similar to naïve animals, 544 proteins were detected in sham animals and 576 proteins at 1hr after HI. To take into consideration that sham-operated animals received isoflurane anesthesia, which might modify the neurotransmitter receptors at PSD, proteins from naïve, sham and HI-injured animals were compared and the ones that were only present under HI condition were selected. These were defined as proteins that are newly recruited into the PSD in response to neonatal HI (Table 2). Proteins that are regulated by calcium were separated because elevated intracellular calcium in postsynaptic neurons from both external influx and internal release following HI is an important regulator of neurotransmitter receptor function and signaling pathways leading to cell death/survival. It mostly involves activation of protein kinases/phosphatases, Ras-family GTPases and their co-players, for example, conventional protein kinase C (PKCα, β and γ), CaMKIV and two proteins implicated in Ras signaling pathways (CNKSR2 and RASGRP2). Calpain-5 is a non-classical member of the calpain family that is highly expressed in the CNS [49], but whether it functions the same way as the other members in synaptic activity and neurotoxixity is unknown. Some proteins are associated with neurite extension/synapse maturation or neuronal viability during neural development (Abl interactor [50,51], gamma-adducin [52,53], FKBP8 [54,55], hippocalcin [56,57], CD47 [58], Nova-1 [59,60], TANC2 [61] and Teneurin [62,63]). And several listed proteins have been reported to participate in cell death mechanisms in adult brain ischemia (Dynamin-1 [64,65], FKBP8 [66], CD47 [67,68] and TDP-43 [69,70]). PIKE-L [71] and Nova-1 [72] have been shown to play roles in neuroprotection and repair after brain ischemia.

Identification of proteins with differential expression early after neonatal HI

To reveal HI-induced changes in protein expression, a comparison was made for the peptide counts from triplicate LC-MS/MS runs for each PSD sample from naïve, sham and post-HI brains. After calculating the mean count ratio of each protein in HI over sham group (HI/sham), proteins whose relative expression (peptide counts) in HI samples were at least 50% higher (ratio ≥ 1.5, Table 3) or 50% lower (ratio ≤ 0.5, Table 4) than those in sham samples were identified. 95% confidence intervals were also included to show reliability of the results. These differentially expressed proteins are mainly involved in kinases/phosphatases,

scaffold/adaptor and membrane trafficking proteins, cytoskeleton and modulators and cell adhesion proteins. HI enhanced the expression of CaMKII, CaMKV, PKA, DCLK2, Fyn, Src kinase signaling inhibitor 1 (SNIP), and protein phosphatase PP1 (Table 3). On the other hand, receptor-type tyrosine-protein phosphatase zeta (R-PTP-zeta, phosphacan), which is restricted to CNS [73] and primarily expressed in neural progenitors and induced in remyelinating oligodendrocytes [74], was down-regulated after HI (Table 4). Expression of Blk, another Src family kinase that was not previously found in the developing brain, was decreased (Table 4). These changes, along with alternations in other proteins, suggest re-wiring of cellular signaling networks and reconstruction of PSD cytoskeleton after neonatal HI, which might be associated with vulnerability to injury or impairment of synaptic plasticity following the insult.

Neonatal HI affects phosphorylation of NMDA receptor subunit NR2B

Validation of some proteins detected in MS experiments with Western blotting was carried out and focused firstly on the NMDA receptors (NMDAR) because NMDAR-mediated excitotoxicity is an early event after HI, and an important contributor of neuronal cell death. It was surprising that NR2A subunit was not detected in the MS runs, possibly due to its significant lower abundance than NR2B in the developing brain. The protein level of PSD NR1 was not affected by HI within the first 24 hours of reperfusion, while expression of NR2A and NR2B decreased over time. Phosphorylation of NR2B, including Fyn-mediated phosphorylation at tyrosine (Y) 1472 and CK2α-mediated phosphorylation at serine (S) 1480 was significantly changed. Y1472 phosphorylation increased at 15min and 1hr after HI (Fig. 2A, B, $p<0.05$, $n=4$), while S1480 phosphorylation gradually decreased at 1hr, 6hr and 24 hr post-HI (Fig. 2A, B, $p<0.05$, $n=4$). Phosphorylation of Y1336, another Fyn target site on NR2B, remained the same. Src kinases, the core glutamate receptor kinases at PSD [75], were profoundly activated as indicated by the increase of their active form pY416 Src (Fig. 2A, C, n=5). Fyn and Src were detected in proteomic analysis, with their protein levels unaffected with HI (Fig. 2A), which is consistent with our previous study [26]. Fyn was found increased in MS analysis (Table 3). Src kinase signaling inhibitor 1 (SNIP or SNAP-25-interacting protein, p130Cas-associated protein), a negative regulator of Src, was upregulated at 1hr (from both MS and Western blotting results), and then declined at 6hr and 24hr after HI (Fig. 2A, C). Casein kinase 1 (CK1) and 2 (CK2) are highly conserved serine/threonine kinases that have a wide variety of substrates, including NR2B. CK1 was identified in the proteomic analysis, but not CK2. The expression of CK1α increased early after HI, while CK2α expression was unchanged (Fig. 2A, D).

Neonatal HI activates multiple signaling kinases at PSD

PSD is considered as a postsynaptic signaling hub where stimulation of neurotransmitter receptors activates multiple and overlapping signaling pathways leading to biochemical and morphological changes of PSD itself and the overall neuronal viability. To investigate how HI would modify these complex networks, the expression of major stress-evoked protein kinases and their phosphorylation status after HI were determined. CaMKIIα was markedly activated early after HI (15min, 1hr and 6hr) as presented as the ratio of (phospho-)pCaMKIIα/total CaMKIIα (Fig.3A, B, $p<0.05$, $n=5$). CaMKIIβ, also neuron-specific and highly enriched in PSD, was upregulated up to 6hrs following HI (Fig.3A, B).

The MS analysis detected translocation of PKCα, β and γ to PSD after HI, which was validated by Western blotting with a robust induction for up to 6hrs as shown in Fig.3A, D ($p<0.05$, n=3). Expression of neuronal nitric oxide synthase (nNOS), an important downstream effector of NR2B-PSD95 complex but undetectable in all postsynaptic proteomics, was increased for at least 24hrs after HI (Fig.3A, B, $p<0.05$, n=5). Phosphatidylinositol-4,5-bisphosphate 3-kinase (PI3K) is also implicated in long-term potentiation and multitudinous cellular function. Its regulatory subunit p85 was found to be persistently overexpressed at PSD after HI (Fig.3A, B, $p<0.05$, n=4). HI induces mitogen-activated protein kinases (MAPKs) including ERK1/2, p38 and JNK kinases. MAPKs are involved in a variety of fundamental cellular processes and have been studied intensively in neonatal brain HI models. It is interesting that ERK and its phosphorylated form (pERK), but not p38, are localized at synapses in sham animals (Fig. 3A, n=4). p38 was translocated into PSD after HI and stayed there for at least 24hrs. ERK2 was activated at PSD early after HI (15min and 1hr) while ERK1 phosphorylation seemed unchanged (Fig. 3A, C, n=4).

Neonatal HI modifies PSD scaffold and adaptor proteins

The neurotransmitter receptors are anchored on the postsynaptic membrane through their interactions with PSD scaffold/adaptor proteins and cytoskeleton proteins. The MS data showed a down-regulation of many scaffold proteins (Table 4) including both presynaptic and postsynaptic proteins that are important for synapse formation and function. The discs large (DLG) subfamily of membrane-associated guanylate kinase (MAGUK) scaffold proteins (PSD95, PSD93, SAP102 and SAP97) links the receptors to intracellular signaling networks. All four MAGUK members were identified and showed reduced expression after HI in proteomic analysis (Table 4). Western blotting validated the decreased post-HI levels of PSD95, PSD93 and SAP102 (Fig. 4, $p < 0.05$, n= 4). The expression of SynGAP, a Ras-GTPase activating protein that interacts with the PDZ domains of PSD95 and SAP102, was decreased at 24 hrs after HI ($p<0.05$, n=4).

Discussion

Recent synaptic proteomic studies in postnatal brain have provided valuable resource for understanding the enhanced plasticity during critical periods and possible synaptic deficits underlying developmental brain disorders [13–15]. The present work focused on profiling postsynaptic density proteins from P9 mouse cortex. A total of 512 PSD proteins were identified, among which 60 proteins have not been reported in previous synaptic proteomic studies. Seven of them are unique for their involvement in neurite maturation and neural development. An episode of hypoxia-ischemia increased the yield of PSD early after HI and triggered translocation of many proteins, including Ca^{2+}-regulated proteins into PSDs. Differentially expressed proteins at 1 hour after HI were tabulated. Validation demonstrated the expression and modification of the NMDA receptor, as one example of neurotransmitter receptors, in response to HI. Activation of a serious of protein kinases that are involved in synaptic transmission or pathways leading to cell death/survival in neonatal model of HI was also seen. Finally, impaired expression of PSD scaffold and adaptor components may suggest a local disassembly or disruption of the postsynaptic apparatus predicting defected plasticity following early brain injury.

Previous postsynaptic proteome have identified several hundreds to more than 2,000 proteins from mouse brain, mostly from whole brain or forebrains [1,4,5,27], while only cortical tissue was used in this study. Instead of the routine in-gel digestion after one- or two-dimensional gel electrophoresis for protein identification with MS, an in-solution digestion procedure was employed to avoid loss of proteins during gel extraction, however, it may also reduce the chances of detecting low abundant proteins, which is a common issue of MS-based proteomic study. The false positive rate for peptide identification was estimated to be 1.2% indicating the reliability of protein identification. The protein profile of PSD from P9 mouse is similar to that of adult brain, consisting of proteins classified in the same functional categories except those with unknown biological functions. This suggests that synapses at this developing stage may have already assembled the majority of proteins as when they mature, although the synapses are still scarce on spines but increase steadily within the first few weeks of rodent life. This is in line with a recent report showing that the same number of synaptic membrane proteins were identified across the ages of P9 to P280 with differences in abundance of many of them over time [13]. Core presynaptic and postsynaptic proteins are revealed at low levels at P9 with an overall increase in expression levels or subunit shift during development [13]. By comparison with existing PSD or synaptic proteomic data, we detected 60 novel proteins, including seven of them that are key regulators of brain development in addition to their recognized roles beyond this stage. These proteins are involved in highly active biological processes in the immature brain, which include neural progenitor proliferation and neurogenesis (BRCA2, CHMP1A, SNF2L1 and TLR3), neuronal migration (JIP1 and MARK1), neurite extension (JIP1, MARK1, SNF2L1 and TLR3), or dendrite/synapse development or functioning (MARK1 and SESTD1). Among these proteins, MARK1 and SESTD1 were proven to be localized at PSDs [41,48], whereas the presence and specific roles for the other five proteins at postsynaptic site require further clarification.

Early brain hypoxia-ischemia led to increased yield and changes in molecular composition of neonatal PSDs by recruiting proteins into PSDs and modifying the expression of proteins that belong to diverse functional categories. As expected, increase in intracellular Ca^{2+} from extra- and intracellular sources following HI activates a variety of kinases/phosphatases and small G-proteins, as shown in Table 2, Table 3 and Fig. 2, Fig. 3, which are essential for signal transduction downstream of postsynaptic neurotransmitter receptors or modification of other intracellular signaling pathways. For example, Src family kinase Fyn and Src, protein kinase C, CaMKII, casein kinases, PI3K kinase and MAP kinases are all able to regulate the function of NMDA receptors by direct phosphorylation and/or modifying their interactions with intracellular binding partners. Activation or translocation of these kinases into PSDs immediately after HI may suggest their involvement in NMDA receptor-mediated glutamate excitotoxicity or enhanced synaptic transmission. NR2B subunit is known to be substrate for CaMKIIα, Src kinase, PKC and CKII. Coordination of these kinases (synergistically or antagonistically), and with synaptic phosphatases is critical for synaptic plasticity. For instance, S1480 phosphorylation by CKII decreases Y1472 phosphorylation by Fyn, which underlies the switch from NR2B to NR2A at synapses during development [76]. Phosphorylation of S1480 was suppressed; with a concomitant increase of Y1472 phosphorylation of NR2B was observed after HI. This may be associated with post-HI brain

damage as we demonstrated previously that sustained enhancement of NR2B phosphorylation at Y1472 is detrimental in neonatal HI [77]. Therefore, dysregulation of well-balanced postsynaptic signaling networks by HI could not only impair the normal synapse functionality and developmental plasticity, but also result in neuronal death and brain damage.

HI-induced changes in protein expression of postsynaptic scaffolds and cytoskeleton-associated proteins is another finding from this proteomic study. MAGUK protein PSD95, PSD93 and SAP102 are downregulated as proved by both MS and Western blotting. This is consistent with an earlier protein sequencing study in adult rat model of transient cerebral ischemia [78]. Among the proteins that are recruited to PSD early after HI, Abl interactor, gamma-adducin, band 4.1-like protein 1 [79], dynamin-1 are all involved in the assembly of actin or spectrin-actin network, the major cytoskeletal components in dendritic spines. These proteins play important roles in maintaining physical integrity and stability of the synapses. As summarized in Table 3 and 4, HI triggered alterations in abundance of numerous cytoskeleton molecules and their modulators. These changes in scaffold and cytoskeleton proteins may be indicative of synapse disassembly/degeneration and dysfunction following neonatal HI.

In conclusion, proteomic profiling of PSD proteins of neonatal mouse brain in this study offers useful information on postsynaptic molecular organization in the developing brain. Early brain injury reflecting on the modifications of PSD includes recruitment of proteins into the apparatus, regulation of neurotransmitter receptor phosphorylation, activation of overlapping postsynaptic kinase signaling molecules and dysregulation of scaffold/adaptors and cytoskeleton proteins. Although these early biochemical changes precede the delayed neuronal death, the contribution of individual protein to injury or defense mechanisms after HI remains to be determined. This work provided additional information to the recent efforts of understanding the molecular mechanisms of synaptic development and plasticity during normal brain maturation, and following early brain injury. With the recent proteomic studies of human neocortex PSDs [80], a comparative proteomic study of human and mouse PSDs [81], and human brain after ischemic stroke [82], it would be feasible to characterize PSDs in developing human brain and in patients suffered from hypoxic-ischemic encephalopathy (HIE), to aid early diagnosis and timely intervention to reduce HIE mortality and long-term adverse consequences.

Supplementary Material

Refer to Web version on PubMed Central for supplementary material.

Acknowledgments

This work was funded by grant from NIH National Institute of Neurological Disorders and Stroke RO1NS084057 (Dr. Jiang). Mass Spectrometry was provided by the Bio-Organic Biomedical Mass Spectrometry Resource at UCSF (A.L. Burlingame, Director) supported by the Biomedical Technology Research Centers program of the NIH National Institute of General Medical Sciences, NIH NIGMS 8P41GM103481.

References

1. Collins MO, Husi H, Yu L, Brandon JM, Anderson CN, Blackstock WP, Choudhary JS, Grant SG. Molecular characterization and comparison of the components and multiprotein complexes in the postsynaptic proteome. J Neurochem. 2006; 97(Suppl 1):16–23. [PubMed: 16635246]
2. Jordan BA, Fernholz BD, Boussac M, Xu C, Grigorean G, Ziff EB, Neubert TA. Identification and verification of novel rodent postsynaptic density proteins. Mol Cell Proteomics. 2004; 3:857–871. [PubMed: 15169875]
3. Li KW, Hornshaw MP, Van Der Schors RC, Watson R, Tate S, Casetta B, Jimenez CR, Gouwenberg Y, Gundelfinger ED, Smalla KH, Smit AB. Proteomics analysis of rat brain postsynaptic density. Implications of the diverse protein functional groups for the integration of synaptic physiology. J Biol Chem. 2004; 279:987–1002. [PubMed: 14532281]
4. Peng J, Kim MJ, Cheng D, Duong DM, Gygi SP, Sheng M. Semiquantitative proteomic analysis of rat forebrain postsynaptic density fractions by mass spectrometry. J Biol Chem. 2004; 279:21003–21011. [PubMed: 15020595]
5. Trinidad JC, Specht CG, Thalhammer A, Schoepfer R, Burlingame AL. Comprehensive identification of phosphorylation sites in postsynaptic density preparations. Mol Cell Proteomics. 2006; 5:914–922. [PubMed: 16452087]
6. Yoshimura Y, Yamauchi Y, Shinkawa T, Taoka M, Donai H, Takahashi N, Isobe T, Yamauchi T. Molecular constituents of the postsynaptic density fraction revealed by proteomic analysis using multidimensional liquid chromatography-tandem mass spectrometry. J Neurochem. 2004; 88:759–768. [PubMed: 14720225]
7. Trinidad JC, Thalhammer A, Specht CG, Lynn AJ, Baker PR, Schoepfer R, Burlingame AL. Quantitative analysis of synaptic phosphorylation and protein expression. Mol Cell Proteomics. 2008; 7:684–696. [PubMed: 18056256]
8. Coba MP, Pocklington AJ, Collins MO, Kopanitsa MV, Uren RT, Swamy S, Croning MD, Choudhary JS, Grant SG. Neurotransmitters drive combinatorial multistate postsynaptic density networks. Sci Signal. 2009; 2:ra19. [PubMed: 19401593]
9. Dieterich DC, Kreutz MR. Proteomics of the Synapse–A Quantitative Approach to Neuronal Plasticity. Mol Cell Proteomics. 2016; 15:368–381. [PubMed: 26307175]
10. Carrette O, Burkhard PR, Hochstrasser DF, Sanchez JC. Age-related proteome analysis of the mouse brain: a 2-DE study. Proteomics. 2006; 6:4940–4949. [PubMed: 16912971]
11. Goswami T, Li X, Smith AM, Luderowski EM, Vincent JJ, Rush J, Ballif BA. Comparative phosphoproteomic analysis of neonatal and adult murine brain. Proteomics. 2012; 12:2185–2189. [PubMed: 22807455]
12. Doubleday PF, Ballif BA. Developmentally-Dynamic Murine Brain Proteomes and Phosphoproteomes Revealed by Quantitative Proteomics. Proteomes. 2014; 2:197–207. [PubMed: 25177544]
13. Gonzalez-Lozano MA, Klemmer P, Gebuis T, Hassan C, van Nierop P, van Kesteren RE, Smit AB, Li KW. Dynamics of the mouse brain cortical synaptic proteome during postnatal brain development. Sci Rep. 2016; 6:35456. [PubMed: 27748445]
14. McClatchy DB, Liao L, Lee JH, Park SK, Yates JR 3rd. Dynamics of subcellular proteomes during brain development. J Proteome Res. 2012; 11:2467–2479. [PubMed: 22397461]
15. Moczulska KE, Pichler P, Schutzbier M, Schleiffer A, Rumpel S, Mechtler K. Deep and precise quantification of the mouse synaptosomal proteome reveals substantial remodeling during postnatal maturation. J Proteome Res. 2014; 13:4310–4324. [PubMed: 25157418]
16. Hu X, Rea HC, Wiktorowicz JE, Perez-Polo JR. Proteomic analysis of hypoxia/ischemia-induced alteration of cortical development and dopamine neurotransmission in neonatal rat. J Proteome Res. 2006; 5:2396–2404. [PubMed: 16944952]
17. Rosenkranz K, May C, Meier C, Marcus K. Proteomic analysis of alterations induced by perinatal hypoxic-ischemic brain injury. J Proteome Res. 2012; 11:5794–5803. [PubMed: 23153068]
18. Yang LJ, Ma DQ, Cui H. Proteomic analysis of immature rat pups brain in response to hypoxia and ischemia challenge. Int J Clin Exp Pathol. 2014; 7:4645–4660. [PubMed: 25197337]

19. Zhou Y, Bhatia I, Cai Z, He QY, Cheung PT, Chiu JF. Proteomic analysis of neonatal mouse brain: evidence for hypoxia- and ischemia-induced dephosphorylation of collapsin response mediator proteins. J Proteome Res. 2008; 7:2507–2515. [PubMed: 18471005]
20. Rice JE 3rd, Vannucci RC, Brierley JB. The influence of immaturity on hypoxic-ischemic brain damage in the rat. Ann Neurol. 1981; 9:131–141. [PubMed: 7235629]
21. Jiang X, Knox R, Pathipati P, Ferriero D. Developmental localization of NMDA receptors, Src and MAP kinases in mouse brain. Neurosci Lett. 2011; 503:215–219. [PubMed: 21896318]
22. Knox R, Zhao C, Miguel-Perez D, Wang S, Yuan J, Ferriero D, Jiang X. Enhanced NMDA receptor tyrosine phosphorylation and increased brain injury following neonatal hypoxia-ischemia in mice with neuronal Fyn overexpression. Neurobiol Dis. 2013; 51:113–119. [PubMed: 23127881]
23. Kim S, Pevzner PA. MS-GF+ makes progress towards a universal database search tool for proteomics. Nat Commun. 2014; 5:5277. [PubMed: 25358478]
24. Old WM, Meyer-Arendt K, Aveline-Wolf L, Pierce KG, Mendoza A, Sevinsky JR, Resing KA, Ahn NG. Comparison of label-free methods for quantifying human proteins by shotgun proteomics. Mol Cell Proteomics. 2005; 4:1487–1502. [PubMed: 15979981]
25. Carlin RK, Grab DJ, Cohen RS, Siekevitz P. Isolation and characterization of postsynaptic densities from various brain regions: enrichment of different types of postsynaptic densities. J Cell Biol. 1980; 86:831–845. [PubMed: 7410481]
26. Jiang X, Mu D, Biran V, Faustino J, Chang S, Rincon CM, Sheldon RA, Ferriero DM. Activated Src kinases interact with the N-methyl-D-aspartate receptor after neonatal brain ischemia. Ann Neurol. 2008; 63:632–641. [PubMed: 18384166]
27. Trinidad JC, Thalhammer A, Specht CG, Schoepfer R, Burlingame AL. Phosphorylation state of postsynaptic density proteins. J Neurochem. 2005; 92:1306–1316. [PubMed: 15748150]
28. Zhang G, Neubert TA, Jordan BA. RNA binding proteins accumulate at the postsynaptic density with synaptic activity. J Neurosci. 2012; 32:599–609. [PubMed: 22238095]
29. Frappart PO, Lee Y, Lamont J, McKinnon PJ. BRCA2 is required for neurogenesis and suppression of medulloblastoma. EMBO J. 2007; 26:2732–2742. [PubMed: 17476307]
30. Tsang HT, Connell JW, Brown SE, Thompson A, Reid E, Sanderson CM. A systematic analysis of human CHMP protein interactions: additional MIT domain-containing proteins bind to multiple components of the human ESCRT III complex. Genomics. 2006; 88:333–346. [PubMed: 16730941]
31. Stauffer DR, Howard TL, Nyun T, Hollenberg SM. CHMP1 is a novel nuclear matrix protein affecting chromatin structure and cell-cycle progression. J Cell Sci. 2001; 114:2383–2393. [PubMed: 11559747]
32. Mochida GH, Ganesh VS, de Michelena MI, Dias H, Atabay KD, Kathrein KL, Huang HT, Hill RS, Felie JM, Rakiec D, Gleason D, Hill AD, Malik AN, Barry BJ, Partlow JN, Tan WH, Glader LJ, Barkovich AJ, Dobyns WB, Zon LI, Walsh CA. CHMP1A encodes an essential regulator of BMI1-INK4A in cerebellar development. Nat Genet. 2012; 44:1260–1264. [PubMed: 23023333]
33. Dajas-Bailador F, Bantounas I, Jones EV, Whitmarsh AJ. Regulation of axon growth by the JIP1-AKT axis. J Cell Sci. 2014; 127:230–239. [PubMed: 24198394]
34. Dajas-Bailador F, Jones EV, Whitmarsh AJ. The JIP1 scaffold protein regulates axonal development in cortical neurons. Curr Biol. 2008; 18:221–226. [PubMed: 18261906]
35. Deng CY, Lei WL, Xu XH, Ju XC, Liu Y, Luo ZG. JIP1 mediates anterograde transport of Rab10 cargos during neuronal polarization. J Neurosci. 2014; 34:1710–1723. [PubMed: 24478353]
36. Mandelkow EM, Thies E, Trinczek B, Biernat J, Mandelkow E. MARK/PAR1 kinase is a regulator of microtubule-dependent transport in axons. J Cell Biol. 2004; 167:99–110. [PubMed: 15466480]
37. Maussion G, Carayol J, Lepagnol-Bestel AM, Tores F, Loe-Mie Y, Milbreta U, Rousseau F, Fontaine K, Renaud J, Moalic JM, Philippi A, Chedotal A, Gorwood P, Ramoz N, Hager J, Simonneau M. Convergent evidence identifying MAP/microtubule affinity-regulating kinase 1 (MARK1) as a susceptibility gene for autism. Hum Mol Genet. 2008; 17:2541–2551. [PubMed: 18492799]

38. Biernat J, Wu YZ, Timm T, Zheng-Fischhofer Q, Mandelkow E, Meijer L, Mandelkow EM. Protein kinase MARK/PAR-1 is required for neurite outgrowth and establishment of neuronal polarity. Mol Biol Cell. 2002; 13:4013–4028. [PubMed: 12429843]
39. Reiner O, Sapir T. Mark/Par-1 marking the polarity of migrating neurons. Adv Exp Med Biol. 2014; 800:97–111. [PubMed: 24243102]
40. Wu Q, DiBona VL, Bernard LP, Zhang H. The polarity protein partitioning-defective 1 (PAR-1) regulates dendritic spine morphogenesis through phosphorylating postsynaptic density protein 95 (PSD-95). J Biol Chem. 2012; 287:30781–30788. [PubMed: 22807451]
41. Kwan V, Meka DP, White SH, Hung CL, Holzapfel NT, Walker S, Murtaza N, Unda BK, Schwanke B, Yuen RK, Habing K, Milsom C, Hope KJ, Truant R, Scherer SW, Calderon de Anda F, Singh KK. DIXDC1 Phosphorylation and Control of Dendritic Morphology Are Impaired by Rare Genetic Variants. Cell Rep. 2016; 17:1892–1904. [PubMed: 27829159]
42. Barak O, Lazzaro MA, Lane WS, Speicher DW, Picketts DJ, Shiekhattar R. Isolation of human NURF: a regulator of Engrailed gene expression. EMBO J. 2003; 22:6089–6100. [PubMed: 14609955]
43. Cameron JS, Alexopoulou L, Sloane JA, DiBernardo AB, Ma Y, Kosaras B, Flavell R, Strittmatter SM, Volpe J, Sidman R, Vartanian T. Toll-like receptor 3 is a potent negative regulator of axonal growth in mammals. J Neurosci. 2007; 27:13033–13041. [PubMed: 18032677]
44. Yip DJ, Corcoran CP, Alvarez-Saavedra M, DeMaria A, Rennick S, Mears AJ, Rudnicki MA, Messier C, Picketts DJ. Snf2l regulates Foxg1-dependent progenitor cell expansion in the developing brain. Dev Cell. 2012; 22:871–878. [PubMed: 22516202]
45. Lathia JD, Okun E, Tang SC, Griffioen K, Cheng A, Mughal MR, Laryea G, Selvaraj PK, ffrench-Constant C, Magnus T, Arumugam TV, Mattson MP. Toll-like receptor 3 is a negative regulator of embryonic neural progenitor cell proliferation. J Neurosci. 2008; 28:13978–13984. [PubMed: 19091986]
46. Okun E, Griffioen K, Barak B, Roberts NJ, Castro K, Pita MA, Cheng A, Mughal MR, Wan R, Ashery U, Mattson MP. Toll-like receptor 3 inhibits memory retention and constrains adult hippocampal neurogenesis. Proc Natl Acad Sci U S A. 2010; 107:15625–15630. [PubMed: 20713712]
47. Plant TD, Schaefer M. TRPC4 and TRPC5: receptor-operated Ca2+-permeable nonselective cation channels. Cell Calcium. 2003; 33:441–450. [PubMed: 12765689]
48. Lee CC, Huang CC, Hsu KS. The phospholipid-binding protein SESTD1 negatively regulates dendritic spine density by interfering with Rac1-Trio8 signaling pathway. Sci Rep. 2015; 5:13250. [PubMed: 26272757]
49. Singh R, Brewer MK, Mashburn CB, Lou D, Bondada V, Graham B, Geddes JW. Calpain 5 is highly expressed in the central nervous system (CNS), carries dual nuclear localization signals, and is associated with nuclear promyelocytic leukemia protein bodies. J Biol Chem. 2014; 289:19383–19394. [PubMed: 24838245]
50. Courtney KD, Grove M, Vandongen H, Vandongen A, LaMantia AS, Pendergast AM. Localization and phosphorylation of Abl-interactor proteins, Abi-1 and Abi-2, in the developing nervous system. Mol Cell Neurosci. 2000; 16:244–257. [PubMed: 10995551]
51. Park E, Chi S, Park D. Activity-dependent modulation of the interaction between CaMKIIalpha and Abi1 and its involvement in spine maturation. J Neurosci. 2012; 32:13177–13188. [PubMed: 22993434]
52. Pielage J, Bulat V, Zuchero JB, Fetter RD, Davis GW. Hts/Adducin controls synaptic elaboration and elimination. Neuron. 2011; 69:1114–1131. [PubMed: 21435557]
53. Stevens RJ, Littleton JT. Synaptic growth: dancing with adducin. Curr Biol. 2011; 21:R402–405. [PubMed: 21601803]
54. Edlich F, Maestre-Martinez M, Jarczowski F, Weiwad M, Moutty MC, Malesevic M, Jahreis G, Fischer G, Lucke C. A novel calmodulin-Ca2+ target recognition activates the Bcl-2 regulator FKBP38. J Biol Chem. 2007; 282:36496–36504. [PubMed: 17942410]
55. Shirane M, Ogawa M, Motoyama J, Nakayama KI. Regulation of apoptosis and neurite extension by FKBP38 is required for neural tube formation in the mouse. Genes Cells. 2008; 13:635–651. [PubMed: 18459960]

56. Dovgan AV, Cherkas VP, Stepanyuk AR, Fitzgerald DJ, Haynes LP, Tepikin AV, Burgoyne RD, Belan PV. Decoding glutamate receptor activation by the Ca2+ sensor protein hippocalcin in rat hippocampal neurons. Eur J Neurosci. 2010; 32:347–358. [PubMed: 20704590]
57. Saitoh S, Takamatsu K, Kobayashi M, Noguchi T. Expression of hippocalcin in the developing rat brain. Brain Res Dev Brain Res. 1994; 80:199–208. [PubMed: 7955346]
58. Murata T, Ohnishi H, Okazawa H, Murata Y, Kusakari S, Hayashi Y, Miyashita M, Itoh H, Oldenborg PA, Furuya N, Matozaki T. CD47 promotes neuronal development through Src- and FRG/Vav2-mediated activation of Rac and Cdc42. J Neurosci. 2006; 26:12397–12407. [PubMed: 17135401]
59. Jensen KB, Dredge BK, Stefani G, Zhong R, Buckanovich RJ, Okano HJ, Yang YY, Darnell RB. Nova-1 regulates neuron-specific alternative splicing and is essential for neuronal viability. Neuron. 2000; 25:359–371. [PubMed: 10719891]
60. Ule J, Ule A, Spencer J, Williams A, Hu JS, Cline M, Wang H, Clark T, Fraser C, Ruggiu M, Zeeberg BR, Kane D, Weinstein JN, Blume J, Darnell RB. Nova regulates brain-specific splicing to shape the synapse. Nat Genet. 2005; 37:844–852. [PubMed: 16041372]
61. Han S, Nam J, Li Y, Kim S, Cho SH, Cho YS, Choi SY, Choi J, Han K, Kim Y, Na M, Kim H, Bae YC, Choi SY, Kim E. Regulation of dendritic spines, spatial memory, and embryonic development by the TANC family of PSD-95-interacting proteins. J Neurosci. 2010; 30:15102–15112. [PubMed: 21068316]
62. Tucker RP, Kenzelmann D, Trzebiatowska A, Chiquet-Ehrismann R. Teneurins: transmembrane proteins with fundamental roles in development. Int J Biochem Cell Biol. 2007; 39:292–297. [PubMed: 17095284]
63. Young TR, Leamey CA. Teneurins: important regulators of neural circuitry. Int J Biochem Cell Biol. 2009; 41:990–993. [PubMed: 18723111]
64. Chen YH, Chiang YH, Ma HI. Analysis of spatial and temporal protein expression in the cerebral cortex after ischemia-reperfusion injury. J Clin Neurol. 2014; 10:84–93. [PubMed: 24829593]
65. Kim JY, Kim N, Zheng Z, Lee JE, Yenari MA. 70-kDa Heat Shock Protein Downregulates Dynamin in Experimental Stroke: A New Therapeutic Target? Stroke. 2016; 47:2103–2111. [PubMed: 27387989]
66. Edlich F, Weiwad M, Wildemann D, Jarczowski F, Kilka S, Moutty MC, Jahreis G, Lucke C, Schmidt W, Striggow F, Fischer G. The specific FKBP38 inhibitor N-(N′, N′-dimethylcarboxamidomethyl)cycloheximide has potent neuroprotective and neurotrophic properties in brain ischemia. J Biol Chem. 2006; 281:14961–14970. [PubMed: 16547004]
67. Jin G, Tsuji K, Xing C, Yang YG, Wang X, Lo EH. CD47 gene knockout protects against transient focal cerebral ischemia in mice. Exp Neurol. 2009; 217:165–170. [PubMed: 19233173]
68. Xing C, Lee S, Kim WJ, Jin G, Yang YG, Ji X, Wang X, Lo EH. Role of oxidative stress and caspase 3 in CD47-mediated neuronal cell death. J Neurochem. 2009; 108:430–436. [PubMed: 19012741]
69. Kanazawa M, Kakita A, Igarashi H, Takahashi T, Kawamura K, Takahashi H, Nakada T, Nishizawa M, Shimohata T. Biochemical and histopathological alterations in TAR DNA-binding protein-43 after acute ischemic stroke in rats. J Neurochem. 2011; 116:957–965. [PubMed: 20557425]
70. Shindo A, Yata K, Sasaki R, Tomimoto H. Chronic cerebral ischemia induces redistribution and abnormal phosphorylation of transactivation-responsive DNA-binding protein-43 in mice. Brain Res. 2013; 1533:131–140. [PubMed: 23954745]
71. Liu Z, Jang SW, Liu X, Cheng D, Peng J, Yepes M, Li XJ, Matthews S, Watts C, Asano M, Hara-Nishimura I, Luo HR, Ye K. Neuroprotective actions of PIKE-L by inhibition of SET proteolytic degradation by asparagine endopeptidase. Mol Cell. 2008; 29:665–678. [PubMed: 18374643]
72. Li H, Sun C, Wang Y, Gao Y, Liu Y, Gao Y, Li X, Zhang C. Dynamic expression pattern of neuro-oncological ventral antigen 1 (Nova1) in the rat brain after focal cerebral ischemia/reperfusion insults. J Histochem Cytochem. 2013; 61:45–54. [PubMed: 23042482]
73. Levy JB, Canoll PD, Silvennoinen O, Barnea G, Morse B, Honegger AM, Huang JT, Cannizzaro LA, Park SH, Druck T, et al. The cloning of a receptor-type protein tyrosine phosphatase expressed in the central nervous system. J Biol Chem. 1993; 268:10573–10581. [PubMed: 8387522]

74. Nandi S, Cioce M, Yeung YG, Nieves E, Tesfa L, Lin H, Hsu AW, Halenbeck R, Cheng HY, Gokhan S, Mehler MF, Stanley ER. Receptor-type protein-tyrosine phosphatase zeta is a functional receptor for interleukin-34. J Biol Chem. 2013; 288:21972–21986. [PubMed: 23744080]

75. Zhang F, Guo A, Liu C, Comb M, Hu B. Phosphorylation and assembly of glutamate receptors after brain ischemia. Stroke. 2013; 44:170–176. [PubMed: 23212166]

76. Sanz-Clemente A, Matta JA, Isaac JT, Roche KW. Casein kinase 2 regulates the NR2 subunit composition of synaptic NMDA receptors. Neuron. 2010; 67:984–996. [PubMed: 20869595]

77. Knox R, Brennan-Minnella AM, Lu F, Yang D, Nakazawa T, Yamamoto T, Swanson RA, Ferriero DM, Jiang X. NR2B phosphorylation at tyrosine 1472 contributes to brain injury in a rodent model of neonatal hypoxia-ischemia. Stroke. 2014; 45:3040–3047. [PubMed: 25158771]

78. Hu BR, Park M, Martone ME, Fischer WH, Ellisman MH, Zivin JA. Assembly of proteins to postsynaptic densities after transient cerebral ischemia. J Neurosci. 1998; 18:625–633. [PubMed: 9425004]

79. Gimm JA, An X, Nunomura W, Mohandas N. Functional characterization of spectrin-actin-binding domains in 4.1 family of proteins. Biochemistry. 2002; 41:7275–7282. [PubMed: 12044158]

80. Bayes A, van de Lagemaat LN, Collins MO, Croning MD, Whittle IR, Choudhary JS, Grant SG. Characterization of the proteome, diseases and evolution of the human postsynaptic density. Nat Neurosci. 2011; 14:19–21. [PubMed: 21170055]

81. Bayes A, Collins MO, Croning MD, van de Lagemaat LN, Choudhary JS, Grant SG. Comparative study of human and mouse postsynaptic proteomes finds high compositional conservation and abundance differences for key synaptic proteins. PLoS One. 2012; 7:e46683. [PubMed: 23071613]

82. Cuadrado E, Rosell A, Colome N, Hernandez-Guillamon M, Garcia-Berrocoso T, Ribo M, Alcazar A, Ortega-Aznar A, Salinas M, Canals F, Montaner J. The proteome of human brain after ischemic stroke. J Neuropathol Exp Neurol. 2010; 69:1105–1115. [PubMed: 20940630]

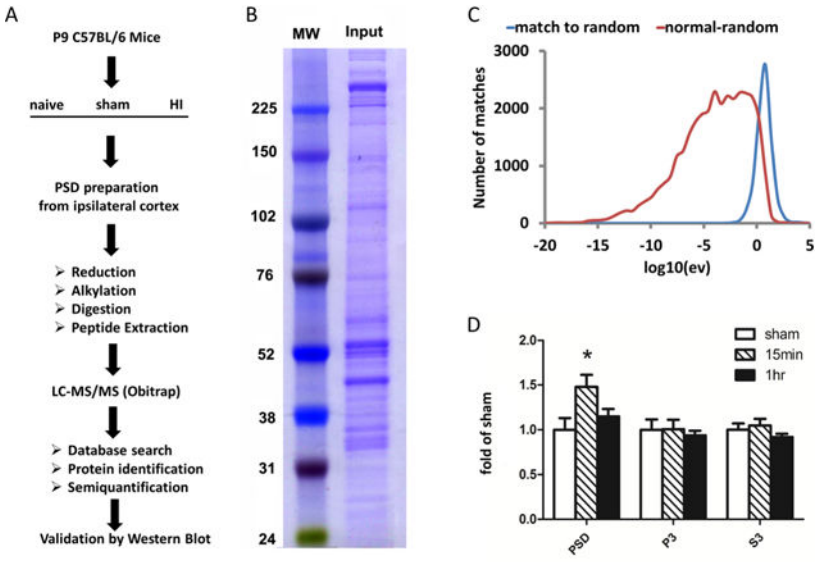

Fig. 1.

A: Schematic representation of the experimental workflow. **B:** Coomassie blue-stained SDS-polyacrylamide gel lane containing purified P9 mouse cortex PSD proteins. A rainbow protein molecular weight (MW) ladder is shown on the left, and a representative PSD sample (input) gel is shown on the right. **C:** The true (red curve) and false (blue curve) distributions of expectation values (e-values) of spectra matched against the SwissProt database. The false match (or random match) distribution was obtained using matches against the randomized version of the normal database. The true match distribution is the subtraction of matches against the normal database from the random matches. The false-positive rate for the MS database search was estimated to be ≈1.2% with the maximal peptide e-value of 0.102. **D:** Yield of PSD, intracellular light membrane (P3), and cytoplasmic proteins (S3) in sham and HI-injured mice at 15 min and 1 h after HI injury. Data are expressed as means ± SD and normalized to the sham values (fold of sham). There is a significant increase in protein yield of PSD at 15 min compared to sham animals (* $p < 0.05$, $n = 8–9$).

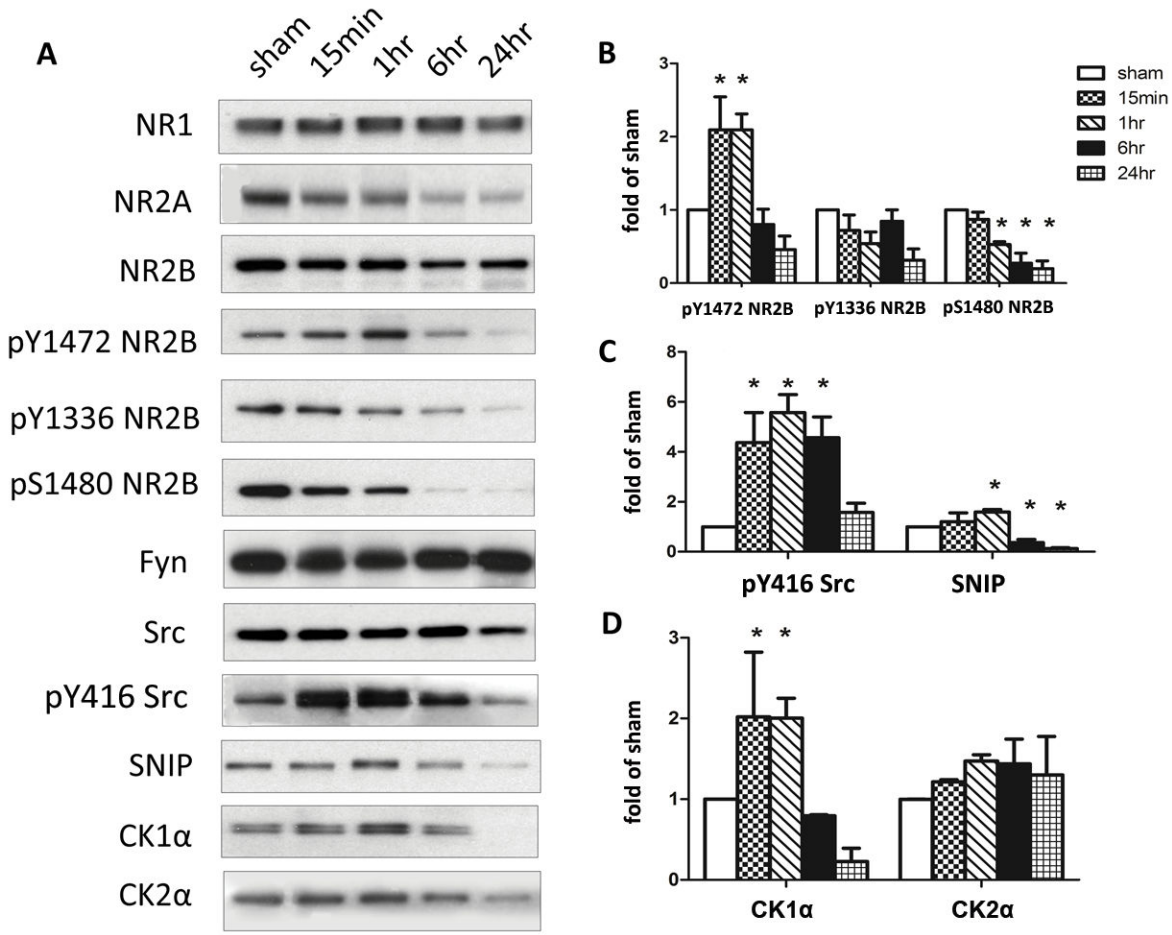

Fig. 2.

Western blotting of NMDA receptor, phosphorylation of NR2B subunit, Src family kinase (Fyn, Src and activated form pY416 Src), Src kinase signaling inhibitor 1 (SNIP) and casein kinase (CK1α and CK2α) at different time point after HI. The levels of protein expression are presented as mean ± SD of the OD values of the blots and normalized to the sham values (fold of sham). *: $p<0.05$ compared to sham (n= 4–5).

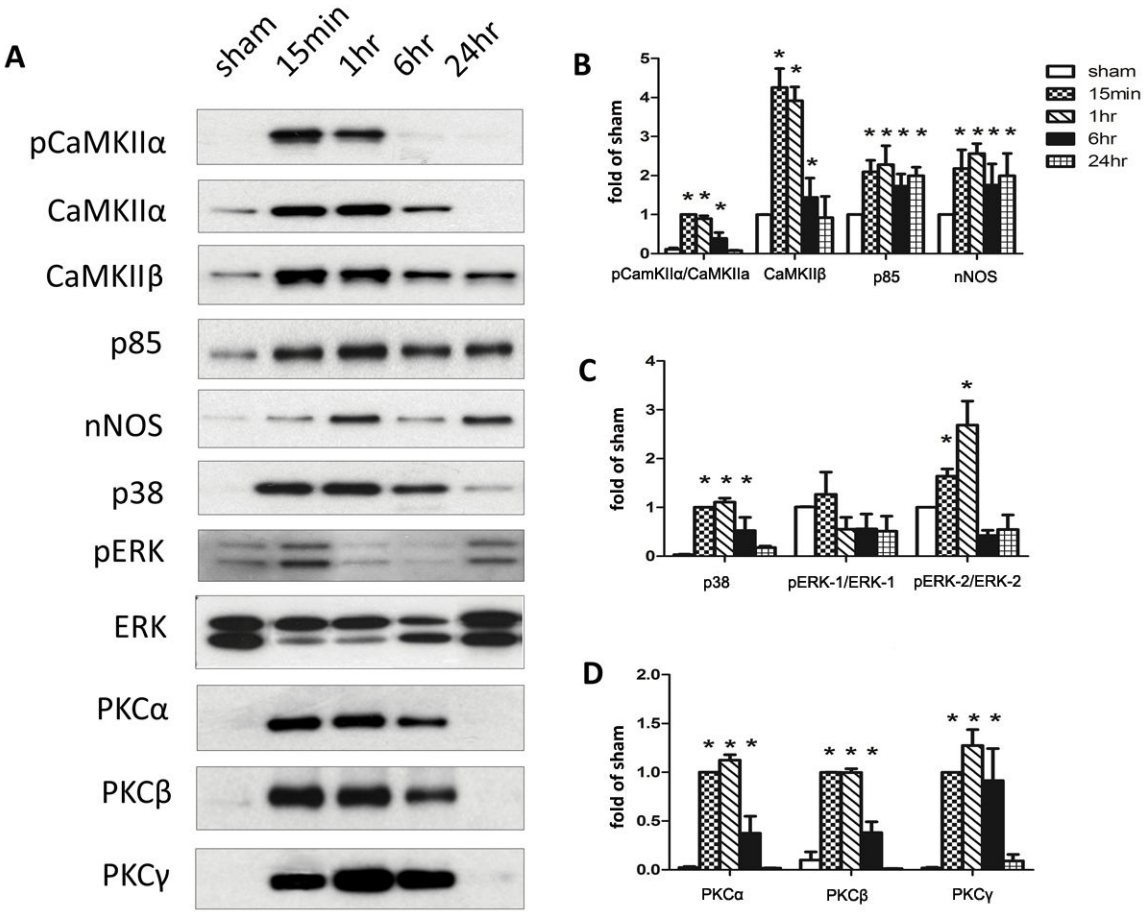

Fig. 3.

Neonatal HI injury activates multiple signaling kinases at PSDs. The antibodies used are listed on the left side of the blots. The levels of protein expression are presented as means ± SD of the OD values of the blots and normalized to the sham values (fold of sham). The protein levels of pCaMKIIα/CaMKIIα, p38, and PKCα, β, and γ were normalized to the values of 15 min. * $p < 0.05$ compared to sham ($n = 4–5$).

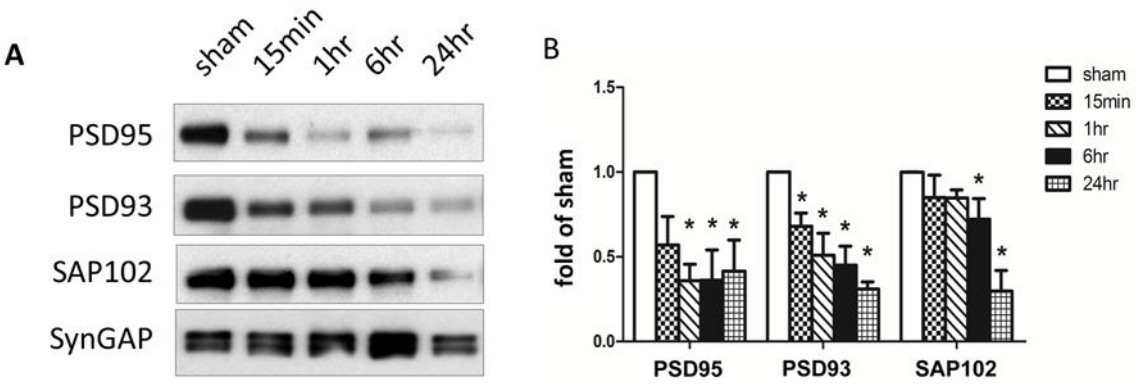

Fig. 4.

Neonatal HI modifies MAGUK family scaffold and adaptor proteins. The antibodies used are listed on the left side of the blots. The levels of protein expression are presented as mean ± SD of the OD values of the blots and normalized to the sham values (fold of sham). *: $p<0.05$ compared to sham (n= 4–5).

Table 1

Newly identified PSD proteins that regulate neural development

Acc #	Protein Name	# unique	% coverage	Expect. Value	Function in the Brain
P97929	Breast cancer type 2 susceptibility protein homolog (BRCA2)	1	0.2	7.60E-03	Regulates apoptosis and neurogenesis during embryonic and postnatal neural development, deficiency leads to microcephaly
Q921W0	Charged multivesicular body protein 1a (CHMP1A)	1	4.6	7.79E-02	Regulates neural progenitor cell proliferation, deficiency leads to pontocerebellar hypoplasia and microcephaly
Q9WVI9	C-Jun-amino-terminal kinase-interacting protein 1 (JIP1)	1	1.6	7.70E-02	Collaborates with AKT to promote axon growth Required for neuronal polarization and migration
Q8VHJ5	Serine/threonine-protein kinase MARK1	1	2.6	6.21E-03	Polarity protein involved in axon – dendrite specification, neurite outgrowth and neuronal migration Regulates dendrite and spine development and functioning Overexpressed in a prefrontal region in autism patients
Q6PGB8	Probable global transcription activator SNF2L1	1	1.1	4.5E-02	Potentiates neurite outgrowth Inhibit progenitor cell expansion Promote neuronal differentiation
Q80UK0	Sec 14 domain and spectrin repeat-containing protein 1 (SESTD1)	1	1.1	3.52E-02	Negatively regulates dendritic spine density Reduces excitotory synaptic transmission in hippocampal neurons
Q99MB1	Toll-like receptor 3 (TLR3)	1	1.1	2.10E-02	Constrains neural progenitor cell proliferation and adult hippocampal neurogenesis Negative regulator of axonal growth in DRG neurons Inhibits hippocampus-dependent learning and memory

The identified proteins are reported with their UniProt accession number (Acc#), name, number of unique peptides used to identify the protein (# unique), percent sequence coverage for the protein (% coverage), the best expectation values for the most confident peptide identification for each protein (Expect. Value) and function in the brain. DRG, dorsal root ganglion

Table 2

Proteins recruited to PSDs early (1hr) after neonatal HI

Acc #	Protein Name	# unique	% coverage	Expect. Value
2A: Calcium-regulated proteins				
Q8CBW3	Abl interactor 1	1	3.33	1.44E-07
P62484	Abl interactor 2	1	3.59	1.13E-06
P08414	Calcium/calmodulin-dependent protein kinase type IV	2	7.25	2.70E-08
O08688	Calpain-5	1	2.81	1.43E-03
Q80YA9	Connector enhancer of kinase suppressor of ras 2 (CNKSR2)	2	2.81	1.24E-06
Q9QYB5	Gamma-adducin	2	4.25	1.95E-10
P84075	Neuron-specific calcium-binding protein hippocalcin	1	4.10	2.00E-03
O35465	Peptidyl-prolyl cis-trans isomerase FKBP8	1	3.98	2.34E-03
P20444	Protein kinase C alpha type	6	10.30	2.50E-05
P68404	Protein kinase C beta type	2	4.92	2.91E-02
P63318	Protein kinase C gamma type	16	35.90	2.60E-09
Q9EQZ6	Rap guanine nucleotide exchange factor 4	1	1.58	1.13E-03
Q9QUG9	RAS guanyl-releasing protein 2 (RASGRP2)	3	9.38	4.65E-07
Q9R0N7	Synaptotagmin-7	1	4.47	3.19E-02
2B: Others				
Q3UHD9	Arf-GAP with GTPase, ANK repeat and PH domain-containing protein 2 (PIKE-L)	1	1.35	2.95E-07
Q8VHH5	Arf-GAP with GTPase, ANK repeat and PH domain-containing protein 3	1	2.09	1.60E-04
Q9Z2H5	Band 4.1-like protein 1	3	6.37	2.52E-05
P39053	Dynamin-1	1	1.20	2.70E-05
Q61735	Leukocyte surface antigen CD47	1	4.62	2.45E-03
P22005	Proenkephalin-A precursor	1	2.61	2.07E-02
Q6NZL0	Protein SOGA3	2	2.65	1.65E-07
A2A690	Protein TANC2	1	0.40	7.45E-03
Q9JKN6	RNA-binding protein Nova-1	1	2.76	9.81E-04
Q9QZX7	Serine racemase	1	7.96	4.89E-03
Q7TT50	Serine/threonine-protein kinase MRCK beta	2	2.63	6.17E-05
Q8R570	Synaptosomal-associated protein 47	6	21.55	4.32E-09
Q921F2	TAR DNA-binding protein 43 (TDP-43)	1	3.14	1.36E-06
Q9WTS5	Teneurin-2	2	1.37	1.66E-03

The identified proteins are reported with their UniPro accession number (Acc#), name, number of unique peptides used to identify the protein (# unique), percent sequence coverage for the protein (% coverage), and the best expectation values for the most confident peptide identification for each protein (Expect. Value).

Table 3

Identification of up-regulated proteins at PSDs early (1hr) after neonatal HI

Acc #	Protein Name	Mean peptide counts			Fold change (HI/sham)	95% Confidence interval (±)
		Naive	Sham	HI		
Receptors, Channels and Transporters						
P55096	ATP-binding cassette sub-family D member 3	1.00	1.67	3.67	2.20	2.12
Q14BI2	Metabotropic glutamate receptor 2	0.67	0.67	1.00	1.50	1.47
Q9QYS2	Metabotropic glutamate receptor 3	0.00	0.67	1.00	1.50	3.17
Scaffold/adaptor proteins						
P17427	AP-2 complex subunit alpha-2	5.67	5.33	9.33	1.75	0.54
P84091	AP-2 complex subunit mu	4.33	4.00	8.00	2.00	1.41
Kinase/phosphatase and regulators						
P11798	Calcium/calmodulin-dependent protein kinase type II subunit alpha	22.67	21.67	38.67	1.78	0.16
P28652	Calcium/calmodulin-dependent protein kinase type II subunit beta	26.00	23.00	36.67	1.59	0.47
Q6PHZ2	Calcium/calmodulin-dependent protein kinase type II subunit delta	3.00	2.33	5.67	2.43	0.96
Q923T9	Calcium/calmodulin-dependent protein kinase type II subunit gamma	2.00	3.67	8.33	2.27	0.76
Q3UHL1	CaM kinase-like vesicle-associated protein (CaMKV)	0.33	1.00	11.33	11.33	0.65
P05132	cAMP-dependent protein kinase catalytic subunit alpha	1.00	0.33	1.00	3.00	1.87
P68181	cAMP-dependent protein kinase catalytic subunit beta	0.00	1.00	1.67	1.67	0.65
P12367	cAMP-dependent protein kinase type II-alpha regulatory subunit	0.00	0.33	1.00	3.00	5.88
P31324	cAMP-dependent protein kinase type II-beta regulatory subunit	0.33	1.33	3.67	2.75	2.33
Q6PGN3	Serine/threonine-protein kinase DCLK2	0.67	1.00	2.00	2.00	0.00
P62137	Serine/threonine-protein phosphatase PP1-alpha catalytic subunit	1.67	2.33	6.33	2.71	2.75
Q9QWI6	SRC kinase signaling inhibitor 1	6.00	3.00	14.67	4.89	2.28
P39688	Tyrosine-protein kinase Fyn	1.00	1.00	2.67	2.67	0.65
Small G-protein, GTPase, ATPase and regulators						
F8VPU2	FERM, RhoGEF and pleckstrin domain-containing protein 1 (FARP1)	1.33	2.66	8.67	3.25	1.44
P46460	Vesicle-fusing ATPase (NSF)	0.67	1.00	11.33	11.33	15.18
Cytoskeleton and modulators						
Q9QYC0	Alpha-adducin	2.67	1.67	6.00	3.60	4.41
Q8R5C5	Beta-centractin	2.33	1.67	4.33	2.60	1.80

Acc #	Protein Name	Mean peptide counts			Fold change (HI/sham)	95% Confidence interval (±)
		Naive	Sham	HI		
Q7TMB8	Cytoplasmic FMR1-interacting protein 1	1.67	1.67	3.00	1.80	1.38
Q5SQX6	Cytoplasmic FMR1-interacting protein 2	1.67	1.67	3.33	2.00	1.25
Q9R0P5	Destrin	0.33	0.33	1.00	3.00	5.88
Q9QXZ0	Microtubule-actin cross-linking factor 1	2.33	2.66	4.67	1.75	1.38
P10637	Microtubule-associated protein tau	5.33	5.33	8.00	1.50	0.85
Q9CQV6	Microtubule-associated proteins 1A/1B light chain 3B	0.33	0.66	1.33	2.00	2.94
O88809	Neuronal migration protein doublecortin	2.00	1.66	3.33	2.00	1.82
Q9CWF2	Tubulin beta-2B chain	1.00	1.00	2.33	2.33	0.65
Q9D6F9	Tubulin beta-4A chain	4.67	10.00	20.33	2.03	0.51
P99024	Tubulin beta-5 chain	4.00	12.67	25.67	2.03	0.64
P20152	Vimentin	0.33	0.33	2.67	8.00	17.64
Cell adhesion						
Q80TS3	Adhesion G protein-coupled receptor L3 precursor	0.00	0.33	1.67	5.00	11.76
P15116	Cadherin-2 precursor	0.00	0.33	2.00	6.00	15.15
Q61301	Catenin alpha-2	1.33	1.67	12.33	7.40	5.73
Q02248	Catenin beta-1	3.33	3.33	8.00	2.40	0.47
O35927	Catenin delta-2	0.00	1.00	2.33	2.33	0.65
Q68FD5	Clathrin heavy chain 1	6.33	4.33	31.33	7.23	1.89
P13595	Neural cell adhesion molecule 1	4.33	6.67	12.67	1.90	0.97
P11627	Neural cell adhesion molecule L1	2.00	3.00	5.00	1.67	0.00
Q99PJ0	Neurotrimin	7.00	7.66	13.33	1.74	0.87
Chaperone/protein folding						
P63017	Heat shock cognate 71 kDa protein	29.67	26.00	52.33	2.01	0.28
P17156	Heat shock-related 70 kDa protein 2	5.00	4.33	11.33	2.62	1.59
DNA/nucleus						
Q60899	ELAV-like protein 2	0.67	1.00	2.00	2.00	1.13
P49312	Heterogeneous nuclear ribonucleoprotein A1	2.66	2.66	4.00	1.50	0.79
Q8R081	Heterogeneous nuclear ribonucleoprotein L	1.33	1.33	2.00	1.50	1.58
Q7TMK9	Heterogeneous nuclear ribonucleoprotein Q	2.67	2.67	5.00	1.88	2.08
Q8VEK3	Heterogeneous nuclear ribonucleoprotein U	1.33	3.00	4.67	1.56	0.22

Dev Neurosci. Author manuscript; available in PMC 2018 March 18.

Acc #	Protein Name	Mean peptide counts			Fold change (HI/sham)	95% Confidence interval (±)
		Naive	Sham	HI		
O88569	Heterogeneous nuclear ribonucleoproteins A2/B1	3.00	4.33	8.67	2.00	0.75
P09405	Nucleolin	1.33	0.67	2.67	4.00	8.82
Q99JF8	PC4 and SFRS1-interacting protein	0.00	0.67	1.00	1.50	1.47
Others						
Q99P72	Reticulon-4 (Nogo protein, neurite outgrowth inhibitor)	2.33	0.67	7.33	11.00	11.76
P62984	Ubiquitin-60S ribosomal protein L40 precursor	3.67	4.67	9.67	2.07	0.72

The identified proteins are reported with their UniPro accession number (Acc#), name, the mean peptide counts in naïve, sham, HI samples, the mean fold change (ratio) of peptide counts of HI over sham (HI/sham), and the range (±) for 95% confidence interval.

Table 4

Identification of down-regulated proteins at PSDs early (1hr) after neonatal HI

Acc #	Protein Name	Mean peptide counts			% of sham (HI/sham)	95% Confidence interval (±)
		Naive	Sham	HI		
Receptors, Channels and Transporters						
Q01097	Glutamate receptor ionotropic, NMDA 2B	5.67	9.33	1.00	0.11	0.15
Q8VDN2	Sodium/potassium-transporting ATPase subunit alpha-1	5.67	6.33	2.00	0.32	0.24
Q6PIE5	Sodium/potassium-transporting ATPase subunit alpha-2	1.66	2.00	1.00	0.50	0.00
P14094	Sodium/potassium-transporting ATPase subunit beta-1	2.00	1.67	0.67	0.40	0.94
Kinase/phosphatase and regulators						
B9EKR1	Receptor-type tyrosine-protein phosphatase zeta	2.00	3.00	1.33	0.44	0.39
P16277	Tyrosine-protein kinase Blk	1.00	1.00	0.33	0.33	0.65
Scaffold/adaptor proteins						
Q8BKX1	Brain-specific angiogenesis inhibitor 1-associated protein 2	10.67	9.00	2.33	0.26	0.19
Q811D0	Disks large homolog 1 (SAP97)	1.33	2.67	1.00	0.38	0.09
Q91XM9	Disks large homolog 2 (PSD93)	0.67	0.33	0.00	0.00	0.00
P70175	Disks large homolog 3 (SAP102)	6.00	4.33	0.33	0.08	0.18
Q62108	Disks large homolog 4 (PSD95)	6.33	5.33	0.67	0.13	0.19
Q6PH08	ERC protein 2	5.33	1.67	0.67	0.40	0.96
Q9Z2Y3	Homer protein homolog 1	9.33	9.66	4.00	0.41	0.07
Q80TE7	Leucine-rich repeat-containing protein 7 (Densin-180)	1.33	2.00	0.67	0.33	0.16
O88737	Protein bassoon	3.67	3.00	1.33	0.44	0.77
Q9QYX7	Protein piccolo	2.67	4.00	1.67	0.42	0.44
D3YZU1	SH3 and multiple ankyrin repeat domains protein 1(Shank 1)	0.67	1.67	0.00	0.00	0.00
Q80Z38	SH3 and multiple ankyrin repeat domains protein 2 (Shank 2)	5.67	8.67	1.67	0.19	0.17
Small G-protein, GTPase, ATPase and regulators						
P60766	Cell division control protein 42 homolog	1.67	1.00	0.00	0.00	0.00
P50518	V-type proton ATPase subunit E 1	2.00	1.00	0.00	0.00	0.00
Cytoskeleton and modulators						
P59999	Actin-related protein 2/3 complex subunit 4	1.67	2.67	1.00	0.38	0.09
Q80VC9	Calmodulin-regulated spectrin-associated protein 3	1.00	0.33	0.00	0.00	0.00

Acc #	Protein Name	Mean peptide counts			% of sham (HI/sham)	95% Confidence interval (±)
		Naive	Sham	HI		
Q8BMK4	Cytoskeleton-associated protein 4	11.67	11.67	5.67	0.49	0.26
Q9WV69	Dematin	1.67	1.67	0.67	0.40	0.55
Q5DU25	IQ motif and SEC7 domain-containing protein 2	1.33	0.67	0.33	0.50	0.06
Motor proteins						
Q61595	Kinectin	4.67	5.33	0.00	0.00	0.00
P28740	Kinesin-like protein KIF2A	4.33	2.67	1.00	0.37	0.55
DNA/nucleus						
O70251	Elongation factor 1-beta	5.67	6.00	2.67	0.44	0.19
P57776	Elongation factor 1-delta	2.67	2.67	0.33	0.13	0.28
Q9D8N0	Elongation factor 1-gamma	5.67	10.33	3.67	0.35	0.15
Q9D0E1	Heterogeneous nuclear ribonucleoprotein M	4.00	3.33	1.67	0.50	0.28
Mitochondrial						
O35129	Prohibitin-2	2.33	3.67	1	0.27	0.63
Others						
P04370	Myelin basic protein	2.67	1.50	0	0.00	0.00
Q91V61	Sideroflexin-3	1.00	1.33	0	0.00	0.00

The identified proteins are reported with their UniPro accession number (Acc#), name, the mean peptide counts in naïve, sham, HI samples, the mean ratio (% of sham) of peptide counts of HI over sham (HI/sham), and the range (±) for 95% confidence interval.